Inorganics **2015**, *3*, 40-54; doi:10.3390/inorganics3010040

OPEN ACCESS

inorganics

ISSN 2304-6740

www.mdpi.com/journal/inorganics

Article

Disulfide Competition for Phosphine Gold(I) Thiolates: Phosphine Oxide Formation *vs.* Thiolate Disulfide Exchange

Gamage S. P. Garusinghe, S. Max Bessey, Mostapha Aghamoosa, Meaghan McKinnon, Alice E. Bruce * and Mitchell R. M. Bruce *

Department of Chemistry, University of Maine, Orono, ME 04469-5706, USA;
E-Mails: gamage.garusinghe@umit.maine.edu (G.S.P.G.);
stanley.bessey@umit.maine.edu (S.M.B.); mostapha.aghamoosa@gmail.com (M.A.);
mckinnonme7@gmail.com (M.M.)

* Authors to whom correspondence should be addressed; E-Mails: abruce@maine.edu (A.E.B.); mbruce@maine.edu (M.R.M.B.); Tel.: +1-207-581-1182 (A.E.B.); +1-207-581-1190 (M.R.M.B.); Fax: +1-207-581-1191 (A.E.B. & M.R.M.B.).

Academic Editor: Antonio Laguna

Received: 19 November 2014 / Accepted: 9 February 2015 / Published: 27 February 2015

Abstract: Phosphine gold(I) thiolate complexes react with aromatic disulfides via two pathways: either thiolate–disulfide exchange or a pathway that leads to formation of phosphine oxide. We have been investigating the mechanism of gold(I) thiolate–disulfide exchange. Since the formation of phosphine oxide is a competing reaction, it is important for our kinetic analysis to understand the conditions under which phosphine oxide forms. ^{1}H and ^{31}P{^{1}H} NMR, and GC-MS techniques were employed to study the mechanism of formation of phosphine oxide in reactions of R_3PAu(SR') (R = Ph, Et; SR' = $SC_6H_4CH_3$, SC_6H_4Cl, $SC_6H_4NO_2$, or tetraacetylthioglucose (TATG)) and R*SSR* (SR* = $SC_6H_4CH_3$, SC_6H_4Cl, $SC_6H_4NO_2$, or $SC_6H_3(COOH)(NO_2)$). The phosphine oxide pathway is most significant for disulfides with strongly electron withdrawing groups and in high dielectric solvents, such as DMSO. Data suggest that phosphine does not dissociate from gold(I) prior to reaction with disulfide. 2D (^{1}H-^{1}H) NMR ROESY experiments are consistent with an intermediate in which the disulfide and phosphine gold(I) thiolate are in close proximity. Water is necessary but not sufficient for formation of phosphine oxide since no phosphine oxide forms in acetonitrile, a solvent, which frequently contains water.

Keywords: phosphine gold(I) thiolate; thiolate disulfide exchange; phosphine oxide; ROSEY 2D NMR

1. Introduction

Thiol–disulfide exchange reactions are essential for a number of biochemical transformations. The mechanism of this reaction in solution (in the absence of metals) is described as S_N2 between thiolate and disulfide [1,2]. We have been studying how metals, such as a phosphine gold(I) thiolate complexes, alter the mechanistic reaction pathways for thiol–disulfide exchange. Our work to date has shown that the phosphine gold(I) thiolate–disulfide exchange reaction is overall second order; first order in gold–thiolate and first order in disulfide (see Equation (1)) [3–5]. The initial products of exchange are the unsymmetrical disulfide (*i.e.*, *R**SS*R*′) and a new gold–thiolate complex (*i.e.*, R_3PAuS*R**). In a second step, the unsymmetrical disulfide reacts with the gold–thiolate starting material forming the symmetrical disulfide (*R*′SS*R*′) (see Equation (2)). Furthermore, neither free thiolate nor gold(III) (from possible oxidative addition of disulfide) [6] appear to be involved in the reaction.

$$R_3\text{PAuS}R' + R^*\text{SS}R^* \rightleftarrows R_3\text{PAuS}R^* + R^*\text{SS}R' \quad (1)$$

$$R_3\text{PAuS}R' + R^*\text{SS}R' \rightleftarrows R_3\text{PAuS}R^* + R'\text{SS}R' \quad (2)$$

Our focus has been on understanding how the phosphine and thiolate ligands, disulfide, and solvent influence the kinetics of the exchange reaction. During the course of exchange studies, we have found that the nature of the solvent has a profound effect on the outcome of the reaction. When the reaction is carried out in solvents of low dielectric constant (e.g., methylene chloride), thiolate–disulfide exchange is clean but occurs very slowly (e.g., hours to days timescale). In solvents with higher dielectric constants (e.g., acetonitrile), thiolate–disulfide exchange is faster (e.g., min to hours timescale).

We have reported our preliminary findings on exchange reactions [3–5,7–10], but several issues to date have complicated the data analysis. One has been trace impurities in certain solvents that persist at the low mM concentration and complicate kinetic analysis when metal thiolate disulfide exchange reactions are studied at μM to mM concentrations. This issue will be reported separately [11]. The other issue has been a competing reaction leading to formation of phosphine oxide and a bis-thiolate gold(I) complex. The production of phosphine oxide becomes evident when the exchange reactions in high dielectric solvents are monitored for longer periods of time. We report here a series of experiments conducted to investigate reaction of disulfide with phosphine gold(I) thiolates in order to gain mechanistic insight into the competing pathways of gold(I) thiolate–disulfide exchange and phosphine oxide formation.

2. Results and Discussion

2.1. Phosphine Oxide Formation in DMSO

Reactions of $Ph_3PAu(SC_6H_4CH_3)$ and $(SC_6H_4NO_2)_2$ were monitored by using ^{1}H and ^{31}P NMR spectroscopy. We observed formation of R_3P=O in DMSO and DMF, but not in tetrahydrofuran, methylene chloride, acetone, or acetonitrile. We investigated the reaction in DMSO in more detail to

determine the influence of the phosphine, thiolate and disulfide on the amount of phosphine oxide formed. The reactions of four phosphine gold(I) thiolates (10 mM) with four disulfides (10 mM) were carried out in DMSO-d_6 and monitored by $^{31}P\{^1H\}$ NMR for 12 h. The results are plotted in Figure 1A–D for reactions of $Ph_3PAuSC_6H_4CH_3$, $Ph_3PAuSC_6H_4Cl$, $Ph_3PAuSC_6H_4NO_2$, and $Et_3PAuTATG$ (auranofin), respectively. The percentage of $R_3P{=}O$ was calculated from the ratio of integrals for $R_3P{=}O$ (at 26.5 ppm for R = Ph or 50.8 ppm for R = Et) and R_3PAuSR' (at 39.2 ppm for R = Ph or 40.3 ppm for auranofin). These are the only two signals observed in the ^{31}P NMR spectra during the course of each reaction. Table 1 lists the reactions in decreasing order of extent of phosphine oxide formation at the 75 min. time point for each combination shown in Figure 1. The results show that disulfides with more strongly electron withdrawing groups [DTNB and $(SC_6H_4NO_2)_2$] produce more phosphine oxide. Electron withdrawing groups on the thiolate ligands also increase the extent of $R_3P{=}O$ formation. However the nature of the disulfide appears to have a larger effect. We have noted some variability in reaction rates with different batches of DMSO-d_6, which may originate from differences in water content in the solvent. The experimental results reported in Table 1 were obtained employing the same batch of DMSO-d_6 solvent.

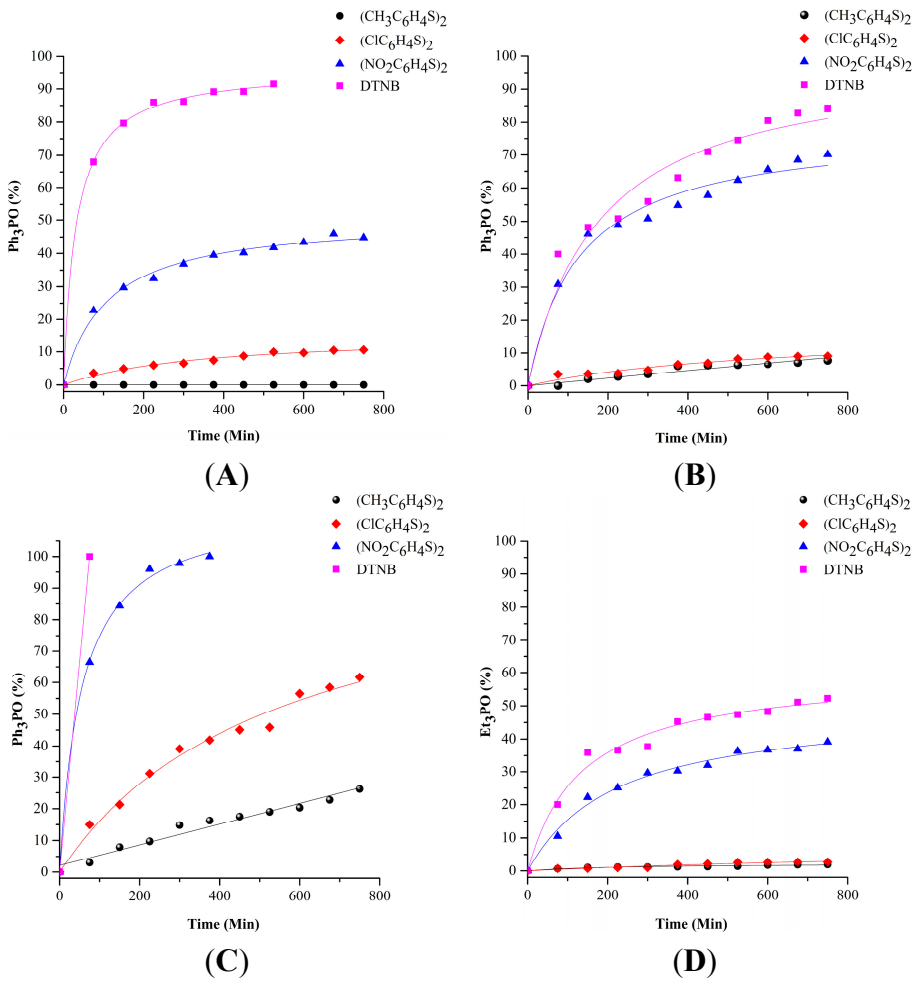

Figure 1. Formation of R_3PO in DMSO-d_6 during reaction of 10 mM disulfides with 10 mM (**A**) $Ph_3PAu(SC_6H_4CH_3)$; (**B**) $Ph_3PAu(SC_6H_4Cl)$; (**C**) $Ph_3PAu(SC_6H_4NO_2)$; (**D**) $Et_3PAu(TATG)$ (auranofin). The percentage of R_3PO was calculated as the ratio of R_3PO to the total phosphorus in the $^{31}P\{^1H\}$ NMR.

Table 1. Comparison of the percentage of $R_3P{=}O$ formed from the reaction of 10 mM PR_3AuSR' and 10 mM *R**SS*R** in DMSO-d_6 (t = 75 min).

R_3PAuSR'	*R**SS*R**	$R_3P{=}O$ (%)
$Ph_3PAuSC_6H_4NO_2$	DTNB [1]	100
$Ph_3PAuSC_6H_4CH_3$	DTNB	68
$Ph_3PAuSC_6H_4NO_2$	$(SC_6H_4NO_2)_2$	67
$Ph_3PAuSC_6H_4Cl$	DTNB	40
$Ph_3PAuSC_6H_4Cl$	$(SC_6H_4NO_2)_2$	31
$Ph_3PAuSC_6H_4CH_3$	$(SC_6H_4NO_2)_2$	23
$Et_3PAu(TATG)$ [2]	DTNB	20
$Ph_3PAuSC_6H_4NO_2$	$(SC_6H_4Cl)_2$	15
$Et_3PAu(TATG)$	$(SC_6H_4NO_2)_2$	11
$Ph_3PAuSC_6H_4CH_3$	$(SC_6H_4Cl)_2$	4
$Ph_3PAuSC_6H_4Cl$	$(SC_6H_4Cl)_2$	3
$Ph_3PAuSC_6H_4NO_2$	$(SC_6H_4CH_3)_2$	3
$Et_3PAu(TATG)$	$(SC_6H_4Cl)_2$	<1
$Et_3PAu(TATG)$	$(SC_6H_4CH_3)_2$	<1
$Ph_3PAuSC_6H_4CH_3$	$(SC_6H_4CH_3)_2$	0
$Ph_3PAuSC_6H_4Cl$	$(SC_6H_4CH_3)_2$	0

[1] DTNB = 5,5'-dithiobis-(2-nitrobenzoic acid); [2] TATG = tetraacetylthioglucose.

2.2. Possible Mechanistic Pathways for Phosphine Oxide Formation in DMSO

Two possible explanations for formation of phosphine oxide are illustrated in Scheme 1. The first involves dissociation of the phosphine ligand from gold(I), followed by nucleophilic attack on disulfide. The second involves reaction of the intact phosphine gold(I) thiolate complex in which the Au-P bond acts as the nucleophile. Dissociation of phosphine from the gold(I) complex was considered likely because of the well-known reaction of triarylphosphines with disulfides. Mechanistic studies reveal that the reaction of Ph_3P and disulfide in dioxane/water mixtures is second order and proceeds via nucleophilic attack of Ph_3P on the S–S bond in disulfide, resulting in a thiophosphonium cationic intermediate ($[R'SPR_3]^+$), which is subsequently hydrolyzed by water to produce phosphine oxide and thiol [12,13]. Disulfides with electron withdrawing groups react faster than those with electron donating groups. We have seen a similar trend for reactions of free Ph_3P with disulfides in DMSO-d_6 solution. For example, reactions of *ca.* 5 mM Ph_3P and 10 mM *R**SS*R** (*R** = $C_6H_4NO_2$, C_6H_4Cl, $C_6H_4CH_3$) were monitored by ^{31}P NMR and the relative rates of formation of $Ph_3P{=}O$ are NO_2 >> Cl > CH_3.

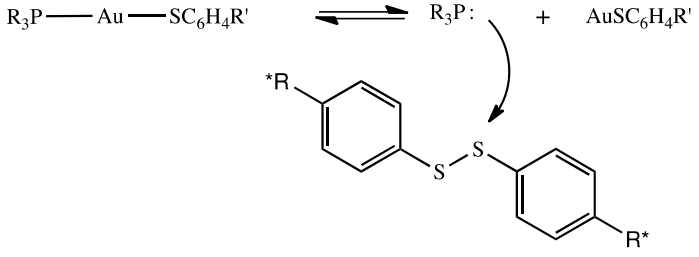

(A)

Scheme 1. *Cont.*

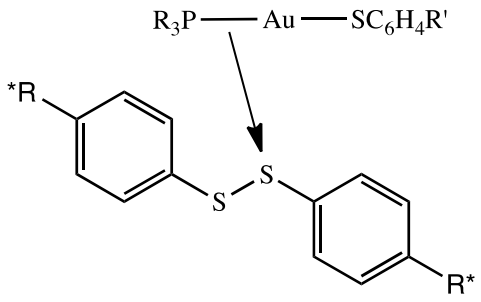

(**B**)

Scheme 1. (**A**) Dissociation of phosphine and nucleophilic attack on disulfide; (**B**) Nucleophilic attack of Au–P bond on disulfide.

It is also interesting to note that $Et_3P=O$ is known to be an *in vivo* metabolite of auranofin. Interactions of auranofin with albumin have been studied *in vitro*. Shaw, *et al.* proposed that Et_3P, from the $Et_3PAu(I)$ moiety bound to the cysteine-34 in albumin, is substituted by an additional cysteine thiolate. The released phosphine reacts with a protein disulfide bond, followed by hydrolysis to give $Et_3P=O$ [14,15].

2.3. No Evidence for Dissociation of Phosphine from Phosphine Gold(I) Thiolate in DMSO

To check for dissociation of phosphine from the phosphine gold(I) thiolate complexes in Table 1, the stability of each gold complex in DMSO-d_6 was monitored by ^1H and ^{31}P NMR. The complexes are stable in this solvent and there is no evidence for dissociation of phosphine over a period of 24 h. An additional check on the stability of the gold–phosphorus bond was performed by adding benzyl azide as a trapping agent [16,17]. In a control reaction, a few drops of neat benzyl azide were added to a 5 mM solution of PPh_3 in DMSO-d_6 and the reaction was observed by ^{31}P NMR. One hour after mixing, all of the phosphine was converted to a mixture of $Ph_3P=O$ and $C_6H_5CH_2N=PPh_3$. In contrast, when a few drops of neat benzyl azide were added to separate solutions of $Ph_3PAuSC_6H_4CH_3$ and $Ph_3PAuSC_6H_4NO_2$ (5 mM in DMSO-d_6), the only peak observed in the ^{31}P NMR was at *ca.* 39 ppm for the Ph_3P ligand in $Ph_3PAu(SR')$. These results suggest that the gold(I) complexes are stable in DMSO-d_6 and phosphine does not dissociate, *i.e.*, the reaction sequence depicted in Scheme 1A is not likely.

2.4. Water Is the Source of Oxygen for the Formation of $Ph_3P=O$

Water is critical to the formation of $R_3P=O$ in the reaction of free phosphine with disulfide. The next set of experiments were carried out to determine whether water is also critical for the formation of $R_3P=O$ in the gold(I)/disulfide system. Dimethyl sulfoxide is a hygroscopic solvent and NMR solutions prepared in the atmosphere typically contain water. We therefore prepared a solution of 10 mM $Ph_3PAuSC_6H_4NO_2$ and 10 mM $NO_2C_6H_4SSC_6H_4NO_2$ in DMSO-d_6 in an argon-filled drybox to minimize the amount of water present. (We used sealed ampoules of 99.5% DMSO-d_6 with a water content of *ca.* 60 ppm, or 3.3 mM). The solution was divided into two portions and a drop of water was added to one of these solutions. Each solution was observed immediately (within 5 min) by ^{31}P NMR. In the solution without added water, approximately 35% of the Ph_3P had been converted to $Ph_3P=O$. Addition of a drop of water (which is an excess) to the second sample caused complete conversion of the phosphine in $Ph_3PAuSC_6H_4NO_2$ to $Ph_3P=O$. This demonstrates that water accelerates the formation of phosphine

oxide in the gold(I)/disulfide system. In addition, GC-MS experiments using labeled water ($H_2{}^{18}O$) demonstrate the formation of $Ph_3P={}^{18}O$, confirming that water is the source of the oxygen in $Ph_3P=O$ (see Experimental Section).

2.5. What Is the Fate of Gold(I)?

When a solution of 7.5 mM $Ph_3PAuSC_6H_4CH_3$ and 5.0 mM $NO_2C_6H_4SSC_6H_4NO_2$ in DMSO-d_6 was monitored by ^1H NMR, a new peak at 7.9 ppm (broad doublet) was observed. This peak was assigned to the aromatic protons in $[Au(SC_6H_4NO_2)_2]^-$ on the basis of comparison to a sample prepared independently by reaction of Au(tht)Cl with two equivalents of the sodium salt of *para*-nitrophenylthiolate ($Na[SC_6H_4NO_2]$).

2.6. Mechanistic Reaction Sequence of Disulfide Competition for Phosphine Gold(I) Thiolates

The competing pathways for formation of thiolate–disulfide exchange and formation of phosphine are summarized in Equations (3)–(7), using as an example the reaction of $Ph_3PAuSC_6H_4CH_3$ and $(SC_6H_4NO_2)_2$.

Thiolate–disulfide exchange:

$$Ph_3PAuSC_6H_4CH_3 + (SC_6H_4NO_2)_2 \rightleftarrows Ph_3PAuSC_6H_4NO_2 + NO_2C_6H_4SSC_6H_4CH_3 \quad (3)$$

Phosphine oxide formation:

$$Ph_3PAuSC_6H_4CH_3 + (SC_6H_4NO_2)_2 \rightleftarrows [Ph_3PSC_6H_4NO_2]^+ + [(NO_2C_6H_4S)Au(SC_6H_4CH_3)\,]^- \quad (4)$$

$$[Ph_3PSC_6H_4NO_2]^+ + H_2O \rightleftarrows Ph_3PO + HSC_6H_4NO_2 + H^+ \quad (5)$$

$$HSC_6H_4NO_2 \rightleftarrows H^+ + [SC_6H_4NO_2]^- \quad (6)$$

$$[SC_6H_4NO_2]^- + [(NO_2C_6H_4S)Au(SC_6H_4CH_3)\,]^- \rightleftarrows [Au(SC_6H_4NO_2)_2]^- + [SC_6H_4CH_3]^- \quad (7)$$

2.7. Scheme 1B Is Supported by 2D (^1H-^1H) NMR Experiments

The second possibility shown in Scheme 1B is that the Au-P bond acts as nucleophile toward the disulfide. Indirect support for this possibility is provided by 2D (^1H-^1H) NMR experiments, described below.

As part of our studies on the mechanism of thiolate–disulfide exchange, we have carried out a series of 2D (^1H-^1H) NMR ROESY experiments. For the self-exchange reaction between $(SC_6H_4NO_2)_2$ and $Ph_3PAuSC_6H_4NO_2$ in CD_3CN during a 12 h ROESY experiment (for which no R_3PO is detected, *vide supra*), analysis of the NOE peaks suggests a close approach of the disulfide and the gold(I)-thiolate moiety, which places the disulfide in a position to undergo exchange with the gold(I) bound thiolate [5]. In addition, on the related zinc(II)-thiolate, disulfide exchange reaction, there is experimental data suggesting close association [5,18], as well as DFT calculations which indicate close association of the disulfide with the zinc(II)-thiolate in the transition state [19].

2.8. 2D (^{1}H-^{1}H) NMR ROESY Experiments

2D (^{1}H-^{1}H) NMR ROESY experiments were also carried out in DMSO-d_6. Since formation of phosphine oxide competes with thiolate–disulfide exchange in this solvent, and leads to eventual decomposition of the gold(I) thiolate complex, reactants were chosen to minimize the formation of R_3PO. On the basis of the results shown in Table 1, we reasoned that the more electron donating methyl substituent on the thiolate ligand and the disulfide would produce the least amount of phosphine oxide. However, a nitro substituent on at least one aromatic ring is desirable because these peaks are well separated from the aromatic ring protons in the thiolate and phosphine ligands (*i.e.*, $SC_6H_4CH_3$ and PPh_3) allowing for easier visualization and assignment of the NOEs. Thus we used $Ph_3PAuSC_6H_4CH_3$ in combination with the unsymmetrical disulfide, $NO_2C_6H_4SSC_6H_4CH_3$. (The unsymmetrical disulfide was prepared *in situ* by mixing $NO_2C_6H_4SSC_6H_4NO_2$ with an excess of $CH_3C_6H_4SSC_6H_4CH_3$, prior to addition of the gold(I) thiolate complex; see experimental section.)

The 2D (^{1}H-^{1}H) NMR ROESY spectrum shown in Figure 2 was acquired over a 4-h period. In this time frame, the starting gold(I) thiolate complex has undergone thiolate–disulfide exchange according to Equation (8). This is evident from the peaks labeled H_3 and H_4, which belong to the thiolate aromatic ring in $Ph_3PAuSC_6H_4NO_2$, and H_1 and H_2 for the nitro aromatic ring in $NO_2C_6H_4SSC_6H_4CH_3$ (see Scheme 2 for labels).

$$Ph_3PAuSC_6H_4CH_3 + NO_2C_6H_4SSC_6H_4CH_3 \rightleftarrows Ph_3PAuSC_6H_4NO_2 + CH_3C_6H_4SSC_6H_4CH_3 \quad (8)$$

The remaining peaks in the 1D ^{1}H-NMR spectra are assigned as follows, starting at the high field side. The intense doublets at 7.38 and 7.18 ppm are due to the large excess of $CH_3C_6H_4SSC_6H_4CH_3$. The doublets at 7.42 and 7.2ppm (partially hidden by the symmetrical disulfide peak at 7.18 ppm) are assigned to the methyl aromatic ring in $NO_2C_6H_4SSC_6H_4CH_3$. The complex multiplet at 7.6 ppm is assigned to PPh_3 and a small amount of Ph_3PO. (The ^{31}P NMR spectrum collected at the end of the 2D (^{1}H-^{1}H) experiment, shows *ca.* 3% $Ph_3P{=}O$ formation, which indicates that the conditions minimize the formation of phosphine oxide.)

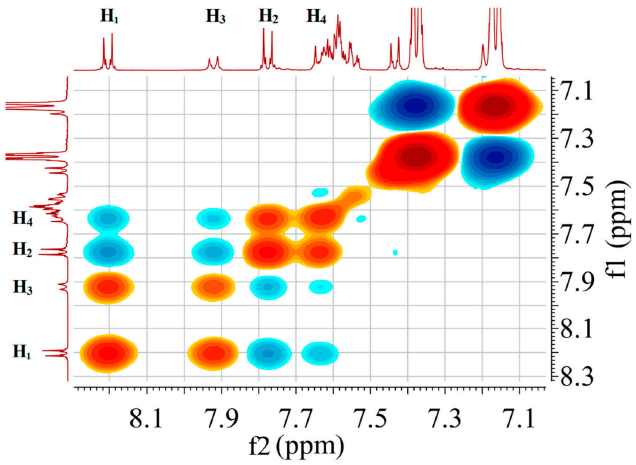

Figure 2. 2D (^{1}H-^{1}H) ROESY spectrum in the aromatic region showing interaction between $Ph_3PAuSC_6H_4NO_2$ and $CH_3C_6H_4SSC_6H_4NO_2$ (DMSO-d_6). See Scheme 2 for assignment of aromatic protons labeled H_1, H_2, H_3, and H_4. (The intense peaks at 7.16 and 7.37 ppm are due to the excess $CH_3C_6H_4S$-$SC_6H_4CH_3$; see Experimental Section.)

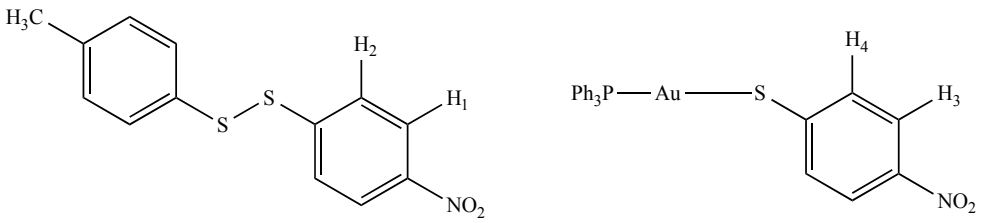

Scheme 2. Labels for aromatic ring protons in the disulfide and gold(I) thiolate complex.

The off diagonal contours in the 2D (^{1}H-^{1}H) ROESY spectrum provide important conformational information. Cross peaks with the same phasing as along the diagonal (red), indicate molecular exchange while the oppositely phased contours (blue) indicate long-range spatial interactions. The red, cross peaks centered at 7.9 and 8.2 ppm indicate thiolate–disulfide exchange between H_3 on the thiolate in $Ph_3PAuSC_6H_4NO_2$ and H_1 on the nitro end of the unsymmetrical disulfide, $NO_2C_6H_4SSC_6H_4CH_3$. (This is a nonproductive exchange since no new molecules are formed.) Intramolecular, long-range interactions between protons on the same ring (ortho to each other) are indicated by blue cross peaks for H_1 and H_2 in the disulfide, and also for H_3 and H_4 on the thiolate.

The most interesting aspect of the 2D (^{1}H-^{1}H) ROESY spectrum is the set of blue cross peaks, which indicate *intermolecular* long-range interactions between H_4 on the thiolate ligand and H_1 on the unsymmetrical disulfide as well as H_3 on thiolate and H_2 on disulfide. The distance between spatially close nuclei can be estimated according to the Equation (9) [20], where η_{ab} is the ROE cross-peak volume (intensity) and r_{ab} is the inter-proton distance of the two protons "a" and "b". The term, r_{ref} is a known distance between two protons and its ROE volume is given by η_{ref} [20].

$$\frac{r_{ab}}{r_{ref}} = \left(\frac{\eta_{ref}}{\eta_{ab}}\right)^{1/6} \quad (9)$$

For our calculation, r_{ref} was chosen as the intramolecular distances between H_1 and H_2 in the disulfide. The crystal structure of the symmetrical disulfide, $(SC_6H_4NO_2)_2$, is available in the Cambridge Structural Database (CSD Refcode: NIPHSS) [21,22] and the average distance between these protons is 2.365 Å. Using this value and the experimental ROE volumes, the spatial separation between H_1…H_4, and H_2…H_3 is estimated to be 2.6 Å.

2.9. Visualizing the Association of Disulfide and the Phosphine Gold(I) Thiolate Complex

Figure 3 shows two views of a cartoon drawing to help visualize the association (and exchange) between disulfide and the phosphine gold(I) thiolate complex. The figure was constructed in Autodesk using typical bond lengths and angles for the disulfide and the gold(I) complex (e.g., the S–S, Au–S, and Au–P bonds are 2.02, 2.30, and 2.26 Å, respectively) [21,23]. The spatial orientations of the two molecules were adjusted to achieve intermolecular H_1…H_4, and H_2…H_3 distances of 2.6 Å, the distance estimated by analysis of the ROESY data. The S–S bond is oriented approximately parallel to the Au–S bond and the intermolecular S…S, S…Au and S…P distances are 3.66, 3.60, and 4.44 Å, respectively. We emphasize that this cartoon is not the result of a calculation but is useful to envision a possible conformational arrangement of the disulfide and gold(I) thiolate complex that is consistent with the ROESY data.

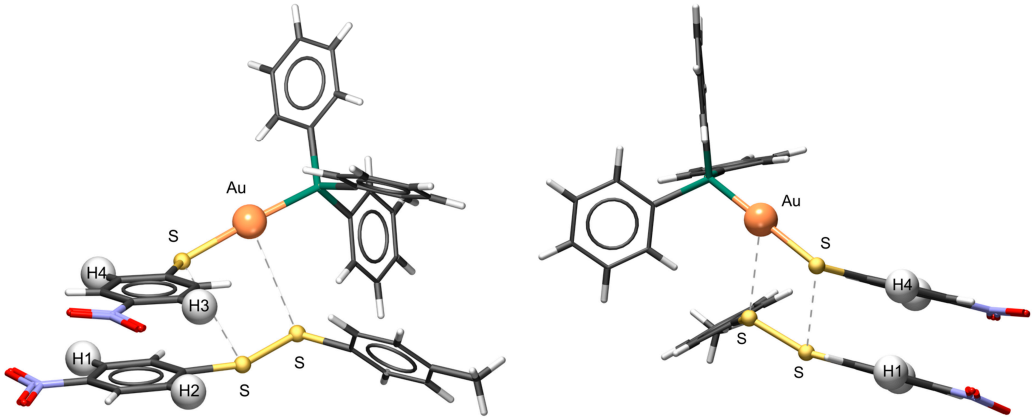

Figure 3. Cartoon drawings in two different views (**A** and **B**) to illustrate a possible orientation of $Ph_3PAu(SC_6H_4NO_2)$ and the unsymmetrical disulfide, $CH_3C_6H_4SSC_6H_4NO_2$. The distance between the aromatic protons, H_1 and H_4, and H_2 and H_3 was set at 2.60 Å. The S…S and Au…S distances are 3.66 and 3.60 Å, respectively. The drawings were generated by using Autodesk 3DS MAX 2013.

Figure 3 also is useful for visualizing the competing reaction that leads to phosphine oxide. Sliding the disulfide along the linear S–Au–P moiety toward the Au–P bond would appear to require a relatively small spatial reorganization and would set up the disulfide to react across the Au–P bond rather than the Au–S bond (see Scheme 3). Reaction of gold(I) with the more electron withdrawing half of the unsymmetrical disulfide is consistent with the known chemistry of gold(I) [24]. The reaction is promoted by DMSO, a solvent with a high dielectric constant (ε = 46.6), which may help to stabilize the charged species that form following scission of the S–S bond.

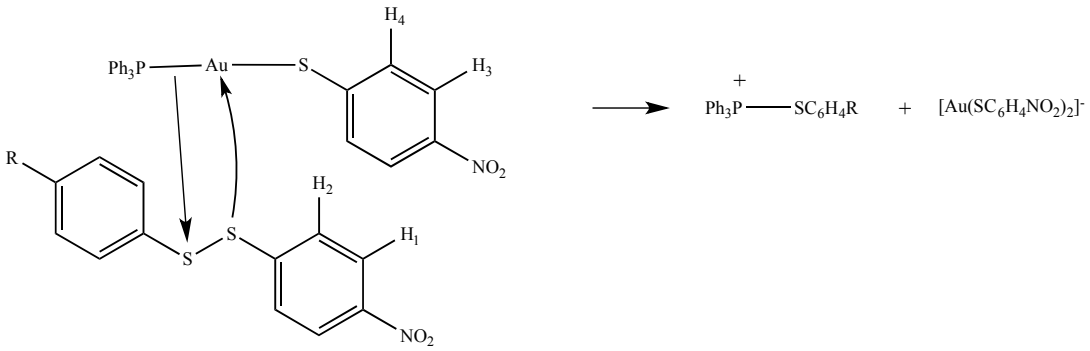

Scheme 3. Competing reaction that leads to phosphine oxide.

3. Experimental Section

3.1. Chemicals and Instrumentation

All NMR solvents were purchased from Cambridge Isotope Laboratories, Inc. (Tewksbury, MA, USA) Only for 2D (^1H-^1H) NMR, solvents in ampules were used as received and solvents in the bottles were used after degassing by 5–10 freeze-pump cycles. Triphenylphosphine oxide (Ph_3PO), triethylphosphine oxide (Et_3PO), triphenylphosphine (PPh_3), benzyl azide (BzN_3), bis(4-chlorophenyl)

disulfide [($ClC_6H_4S)_2$], water ($H_2{}^{18}O$) and Ellman's reagent [5,5′-dithiobis-(2-nitrobenzoic acid) or DTNB] were purchased from Sigma-Aldrich (St. Louis, MO, USA) and used as received. Bis(4-nitrophenyl) disulfide [($O_2NC_6H_4S)_2$] and bis(4-methylphenyl) disulfide [($CH_3C_6H_4S)_2$] were purchased from Sigma-Aldrich (St. Louis, MO, USA) and used after recrystallization. Auranofin [(Et_3P)Au(TATG); TATG = 2,3,4,6-tetraacetyl-1-thio-D-glucopyranosato] was purchased from Enzo Life Sciences (Farmingdale, NY, USA). Syntheses of Au(tht)Cl [25], and phosphine gold(I) thiolates [23], were carried out according to previously reported procedures. Experiments were carried out under atmospheric conditions unless otherwise stated.

$^{31}P\{^1H\}$ NMR spectra were obtained at 26 °C in deuterated solvents on a Varian (Palo Alto, CA, USA) UNITYplus-400 MHz "Oxford" NMR spectrometer operating at 161.9 MHz. $^{31}P\{^1H\}$ NMR spectra were referenced to 85% H_3PO_4 (external standard).

The sample tubes for 2D (^1H-^1H) ROESY (rotating frame Overhauser enhancement spectroscopy) NMR experiments were prepared in a Vacuum Atmospheres dry box under an argon environment and were capped with an air-tight seal. Two-dimensional NMR spectra were acquired at a constant temperature (30 °C) on a Varian (Palo Alto, CA, USA) UNITYplus-400 MHz "Oxford" NMR spectrometer (399.96 MHz for ^1H) equipped with 4-nuc probes. Chemical shifts were referenced to residual ^1H signals of the deuterated solvents.

GC-MS analyses were performed using a Thermo Scientific Trace (Waltham, MA, USA) GC Ultra gas chromatograph and Thermo Scientific (Waltham, MA, USA) ISQ mass spectrometer. Compound separation was achieved with a Rtx5-MS column (30 m × 0.25 mm i.d., crossbond 5% diphenyl/95% dimethyl polysiloxane× 0.25 μm (df) capacity Film thickness, Restek Corp., Bellefonte, PA, USA). The column flow rate was 2 mL/min. The oven temperature was held at 50 °C for 1 min, then increased to 350 °C (at a rate of 20 °C/min) and held at that temperature for 1 min. Injection, MS transfer line, and ion source temperatures were 270, 250, and 200 °C, respectively. Electron ionization mass spectrometric data from *m*/*z* 50 to 300 amu were collected using an ionization voltage of 70 eV. Compound identifications were made by comparing mass spectral patterns with those from known samples and the use of NIST mass spectra database.

3.2. Calibration of ^{31}P NMR Integrals for a Mixture of $Ph_3PAuSC_6H_4CH_3$ and Ph_3PO

The amount of 0.5 mL of a 9.96 mM solution of $Ph_3PAuSC_6H_4CH_3$ in DMSO-d_6 was mixed in a vial with 0.5 mL of a 10.42 mM solution of Ph_3PO in DMSO-d_6. The resulting solution mixture containing 4.98 mM of $Ph_3PAuSC_6H_4CH_3$ and 5.21 mM Ph_3PO was transferred into a NMR tube and investigated by $^{31}P\{^1H\}$NMR experiments. The integral ratio for the peak at 39.2 ppm (Au–P) to the peak at 26.5 (P=O) was *ca.* 1:1.

3.3. Procedure for Measuring % of Phosphine Oxide

The amount of 0.4 mL of a 20.0 mM solution of $Ph_3PAuSC_6H_4R$ (R = CH_3, Cl, NO_2) or Et_3PAu(TATG) in DMSO-d_6 was mixed in a vial with 0.4 mL of a 20.0 mM solution of ($R'C_6H_4S)_2$ (R' = CH_3, Cl, NO_2) or DTNB in DMSO-d_6. The solution mixture containing 10.0 mM $Ph_3PAuSC_6H_4R$ and 10.0 mM ($R'C_6H_4S)_2$ or DTNB was transferred into a NMR tube and investigated by $^{31}P\{^1H\}$ NMR array experiments. The same experimental procedure was carried out for the reaction between

$Et_3PAuSC_6H_4NO_2$ and $(O_2NC_6H_4S)_2$ in DMSO-d_6. The Au–PR_3 peak and R_3P=O peaks were integrated and the % R_3PO is based on the ratio of the R_3P=O integral to the total phosphorus signal.

3.4. Test for Free Phosphine; Reaction of PPh_3 and N_3Bz in DMSO-d_6

Four drops of benzyl azide (N_3Bz) (~1.5 mmol) were added into 0.75 mL of a 5 mM solution of $Ph_3PAuSC_6H_4CH_3$ in DMSO-d_6. $^{31}P\{^1H\}$ NMR spectra were observed over the time. The same reaction was carried out for $Ph_3PAuSC_6H_4NO_2$ in DMSO-d_6. As a control, four drops of benzyl azide (N_3Bz) (~1.5 mmol) were added into 0.75 mL of 5 mM solution of PPh_3 in DMSO-d_6. The $^{31}P\{^1H\}$ NMR spectra were observed over the time.

3.5. Test for Influence of Water

Solutions of $Ph_3PAuSC_6H_4NO_2$ (20 mM) and $(SC_6H_4NO_2)_2$ (20 mM) in DMSO-d_6 were prepared in an argon-filled drybox. Equal volumes of solutions were mixed and the mixture was divided into two NMR tubes. The $^{31}P\{^1H\}$ NMR spectrum was obtained for one sample while keeping the second sample in the drybox. A drop of water was added to the second sample and the $^{31}P\{^1H\}$ NMR spectrum was obtained.

3.6. GC-MS Experiment for Source of Water

The amount of 0.2 mL of $H_2{}^{18}O$ was transferred into 2 mL of DMSO-d_6, which contained 90 ppm (5 mM) water as received from the manufacturer. This solution was used to prepare solutions in the drybox for $^{31}P\ \{^1H\}$ NMR and GC-MS analysis as follows.

A solution of $Ph_3PAuSC_6H_4CH_3$ (5.8 mg in 1.1 mL, 10.0 mM) in DMSO-d_6 was mixed in a vial with a solution of $(O_2NC_6H_4S)_2$ (3.1 mg in 1.1 mL, 10.0 mM) in DMSO-d_6. Then 0.75 mL of the solution mixture was transferred into an NMR tube and investigated by ^{31}P NMR. A separate sample (1 mL) of the same solution was transferred into a vial for GC-MS analysis.

A solution of Ph_3PO in DMSO-d_6 (1.3 mg in 1.0 mL, 4.7 mM) was prepared and analyzed by GC-MS as a reference.

3.7. Reaction of Au(tht)Cl and $Na[SC_6H_4NO_2]$

The reaction was carried out under N_2 using using Schlenk techniques. A solution of sodium methoxide (0.09 g, 1.56 mmol) in CH_3OH (10 mL) was transferred via cannula into a solution of 4-nitrobenzenethiol (0.24 g, 1.56 mmol) in CH_2Cl_2 (20 mL). After stirring at 0 °C for five min., the mixture was transferred into a solution of Au(tht)Cl (0.25 g, 0.78 mmol) in CH_2Cl_2 (20 mL). The final mixture was stirred for 30 mins at 0 °C. The product was obtained by reducing the solvent *in vacuo* and then filtering through a sintered glass crucible in air. The product was washed thoroughly with EtOH and dried under a stream of N_2. Yield calculated for $Na[Au(SC_6H_4NO_2)_2]$: 0.36 g, 90.12%. The sample was dissolved in DMSO-d_6 to obtain a ^1H NMR spectrum. There are two sets of doublets; the set with lower intensity centered at 7.89 and 7.60 ppm appears to convert to a more intense set centered at 7.87 and 7.55 ppm. Over time, the more intense set decreases and no new peaks grow in as a pale yellow solid

precipitates, which is likely a gold(I) thiolate polymer since it is only sparingly soluble in DMSO and insoluble in other solvents.

3.8. 2D (^{1}H-^{1}H) ROESY Experiment

All solutions were prepared in an argon-filled drybox. Preparation of unsymmetrical disulfide: the two symmetrical disulfides, $(SC_6H_4NO_2)_2$ and $(SC_6H_4CH_3)_2$ were combined in an ~1:4 ratio and dissolved in 1 mL of DMSO-d_6. (Complete conversion of $(SC_6H_4NO_2)_2$ to $CH_3C_6H_4SSC_6H_4NO_2$ under these conditions was confirmed by ^{1}H NMR in a separate experiment.) After 30 min, the disulfide mixture was transferred into a vial containing $Ph_3PAu(SC_6H_4CH_3)$. All solids were completely dissolved. The final concentrations of $Ph_3PAu(SC_6H_4NO_2)$, $CH_3C_6H_4SSC_6H_4NO_2$, and $(SC_6H_4CH_3)_2$ at the end of the 2D experiment (~3 h) were estimated by integration to be 20, 30 and 160 mM, respectively. The reaction mixture was transferred into a screw cap NMR tube and a ROESY experiment was carried out with the $\pi/2$–$t1$–$\pi/2$–t_m(spin lock)–$\pi/2$-FID pulse sequence by setting the previously measured PW90 and T_1 for a dummy sample in DMSO-d_6. An 8 s mixing time was applied. The spectra were recorded with 128 increments in $t1$values and 512 data points for the $t2$ dimension with 4 scans per $t1$ increment with a relaxation delay of 3 s. 2D (^{1}H-^{1}H) NMR data were processed with MestReNova NMR software (8.1.1, MestRelab Research, Santiago de Compostela, Spain, 2013).

The cartoon drawing showing a possible orientation of the disulfide and phosphine gold(I) thiolate, which is consistent with the 2D (^{1}H-^{1}H) ROESY experimental results was constructed in Autodesk 3ds MAX (2013, Autodesk, San Rafael, CA, USA).

4. Conclusions

The formation of phosphine oxide in the phosphine gold(I) thiolate–disulfide system shares some features with the reaction of free phosphine and disulfide; *i.e.*, disulfides with electron withdrawing substituents react faster, and water is the source of oxygen. The presence of water is necessary but not sufficient in the gold(I)thiolate–disulfide system since phosphine oxide was not observed in acetonitrile, which also contains mM concentrations of water. There is no evidence for dissociation of the phosphine ligand from the gold(I) complex prior to reaction with disulfide. This suggests that the Au–P bond acts as a nucleophile to attack the S–S bond. 2D (^{1}H-^{1}H) NMR ROESY experiments provide evidence for a close association between disulfide and the gold(I) complex, which we have interpreted as a possible intermediate in the thiolate–disulfide exchange reaction. In addition, we suggest that a small spatial reorganization would allow the disulfide to react with the Au–P bond. The two disulfides which produce the most phosphine oxide are $(SC_6H_4NO_2)_2$ and DTNB. The corresponding thiols of these disulfides have low pKa's (5.5 and 2.95, respectively) [12,26] and the thiolates would be expected to have a strong affinity for gold(I) [24]. This may be an important factor for the formation of the bis-thiolate gold(I) anion shown in Scheme 3. However, the relative affinity of thiolates for gold(I) would also be expected to drive the thiolate–disulfide exchange reaction. Thus the factors controlling the competition between thiolate–disulfide exchange and phosphine oxide formation are subtle and need to be more thoroughly investigated. Finally we have established that phosphine oxide formation happens on a longer time scale than thiolate–disulfide exchange, which is important for kinetic studies aimed at understanding the latter reaction.

Acknowledgments

The authors wish to thank Brian Frederick for his assistance with GC-MS experiments.

Author Contributions

The syntheses, ^{1}H, ^{31}P and 2D NMR experiments were performed by Gamage S. P. Garusinghe. Mostapha Aghamoosa contributed to experiments involving auranofin. Meaghan McKinnon carried reactions of free triphenylphosphine and disulfide. S. Max Bessey constructed Figure 3 and contributed to discussions of the association of disulfide and the phosphine gold(I) thiolate complex. Mitchell R. M. Bruce and Alice E. Bruce supervised the research. Gamage S. P. Garusinghe, Mitchell R. M. Bruce and Alice E. Bruce are responsible for the discussion, analysis of data and writing of the manuscript.

Conflicts of Interest

The authors declare no conflict of interest.

References

1. Whitesides, G.M.; Lilburn, J.E.; Szajewski, R.P. Rates of thiol-disulfide interchange reactions between mono- and dithiols and Ellman's reagent. *J. Org. Chem.* **1977**, *42*, 332–338.
2. Fernandes, P.A.; Ramos, M.J. Theoretical insights into the mechanism for thiol/disulfide exchange. *Chemistry* **2004**, *10*, 257–266.
3. DiLorenzo, M.; Ganesh, S.; Tadayon, L.; Chen, J.; Bruce, M.R.M.; Bruce, A.E. Reactions of organic disulfides and gold(I) complexes. *Met.-Based Drugs* **1999**, *6*, 247–253.
4. Mohamed, A.A.; Abdou, H.E.; Chen, J.; Bruce, A.E.; Bruce, M.R.M. Perspectives in Inorganic and Bioinorganic Gold Sulfur Chemistry. *Comments Inorg. Chem.* **2002**, *23*, 321–334.
5. Garusinghe, G.S.P. Kinetic Analysis of Metal Assisted-Thiolate Disulfide Exchange (*M* = Au, Zn). Ph.D. Thesis, The University of Maine, Orono, ME, USA, May 2013.
6. Bachman, R.E.; Bodolosky-Bettis, S.A.; Pyle, C.J.; Gray, M.A. Reversible Oxidative Addition and Reductive Elimination of Fluorinated Disulfides at Gold(I) Thiolate Complexes: A New Ligand Exchange Mechanism. *J. Am. Chem. Soc.* **2008**, *130*, 14303–14310.
7. Garusinghe, G.S.P.; Bessey, S.M.; Bruce, A.E.; Bruce, M.R.M. Interactions between Metal Thiolate, $R_3PAuSC_6H_4NO_2$ (*R* = Ph and Et) and Bis(4-nitrophenyl) Disulfide. In Proceedings of the 36th Northeast Regional Meeting of the American Chemical Society, Hartford, CT, USA, 7–10 October 2009.
8. Chandrasoma, A.; Bruce, A.; Bruce, M. Insight into Metal-Mediated Thiol–Disulfide Exchange. In Proceedings of the 37th Northeast Regional Meeting of the American Chemical Society, Burlington, VT, USA, 29 June–2 July 2008.
9. Aghamoosa, M.; Briggs, B.; Harriman, E.; Cashman, A.; Bruce, A.; Bruce, M. Gold(I)-Mediated Disulfide Exchange Kinetics as a Function of Solvent Dielectric Constant. In Proceedings of the 37th Northeast Regional Meeting of the American Chemical Society, Burlington, VT, USA, 29 June–2 July 2008.

10. DiLorenzo, M.A.; Ganesh, S.; Bruce, A.E.; Bruce, M.R.M. Gold(I) mediated thiolate/disulfide exchange reactions. In Proceedings of the 213th ACS National Meeting, San Francisco, CA, USA, 13–17 April 1997.
11. Garusinghe, G.S.P.; Bessey, S.M.; Boyd, C.; Aghamoosa, M.; Frederick, B.; Bruce, M.R.M.; Bruce, A.E. (University of Maine, Orono, ME, USA). Determination of dimethyl sulfide in dimethyl sulfoxide. Unpublished work, 2015.
12. Overman, L.E.; Matzinge, D.; Oconnor, E.M.; Overman, J.D. Nucleophilic Cleavage of Sulfur–Sulfur Bond by Phosphorus Nucleophiles—Kinetic Study of Reduction of Aryl Disulfides with Triphenylphosphine and Water. *J. Am. Chem. Soc.* **1974**, *96*, 6081–6089.
13. Dmitrenko, O.; Thorpe, C.; Bach, R.D. Mechanism of SN2 Disulfide Bond Cleavage by Phosphorus Nucleophiles. Implications for Biochemical Disulfide Reducing Agents. *J. Org. Chem.* **2007**, *72*, 8298–8307.
14. Shaw, C.F.; Isab, A.A.; Hoeschele, J.D.; Starich, M.; Locke, J.; Schulteis, P.; Xiao, J. Oxidation of the phosphine from the auranofin analog, triisopropylphosphine(2,3,4,6-tetra-*O*-acetyl-1-thio-β-D-glucopyranosato-*S*)gold(I), via a protein-bound phosphonium intermediate. *J. Am. Chem. Soc.* **1994**, *116*, 2254–2260.
15. Hill, D.T.; Isab, A.A.; Griswold, D.E.; DiMartino, M.J.; Matz, E.D.; Figueroa, A.L.; Wawro, J.E.; DeBrosse, C.; Reiff, W.M.; Elder, R.C.; *et al*. Seleno-Auranofin (Et3PAuSe-tagl): Synthesis, Spectroscopic (EXAFS, ^{197}Au Mossbauer, ^{31}P, ^{1}H, ^{13}C, and ^{77}Se NMR, ESI-MS) Characterization, Biological Activity, and Rapid Serum Albumin-Induced Triethylphosphine Oxide Generation. *Inorg. Chem.* **2010**, *49*, 7663–7675.
16. Lin, F.L.; Hoyt, H.M.; van Halbeek, H.; Bergman, R.G.; Bertozzi, C.R. Mechanistic investigation of the Staudinger ligation. *J. Am. Chem. Soc.* **2005**, *127*, 2686–2695.
17. Woehrle, G.H.; Hutchison, J.E. Thiol-functionalized undecagold clusters by ligand exchange: Synthesis, mechanism, and properties. *Inorg. Chem.* **2005**, *44*, 6149–6158.
18. Boerzel, H.; Koeckert, M.; Bu, W.; Spingler, B.; Lippard, S.J. Zinc-Bound Thiolate-Disulfide Exchange: A Strategy for Inhibiting Metallo-β-Lactamases. *Inorg. Chem.* **2003**, *42*, 1604–1615.
19. Acharige, A. Reactions of Sulfur Compounds with Zn(II), Au(I), and Hg(II) and Metal Linker Polyaniline Electrodes for Energy Storage. Ph.D. Thesis, University of Maine, Orono, ME, USA, May 2011.
20. Binotti, B.; Macchioni, A.; Zuccaccia, C.; Zuccaccia, D. Application of NOE and PGSE NMR methodologies to investigate non-covalent intimate inorganic adducts in solution. *Comments Inorg. Chem.* **2002**, *23*, 417–450.
21. Ricci, J.S.; Bernal, I. Crystal structure of α-bis(*p*-nitrophenyl) disulfide. *J. Am. Chem. Soc.* **1969**, *91*, 4078–4082.
22. Allen, F. The Cambridge Structural Database: A quarter of a million crystal structures and rising. *Acta Crystallogr. Sect. B* **2002**, *58*, 380–388.
23. Narayanaswamy, R.; Young, M.A.; Parkhurst, E.; Ouellette, M.; Kerr, M.E.; Ho, D.M.; Elder, R.C.; Bruce, A.E.; Bruce, M.R.M. Synthesis, structure, and electronic spectroscopy of neutral, dinuclear gold(I) complexes. Gold(I)–gold(I) interactions in solution and in the solid state. *Inorg. Chem.* **1993**, *32*, 2506–2517.

24. Isab, A.A.; Sadler, P.J. A ^{13}C Nuclear Magnetic-Resonance Study of Thiol-Exchange Reactions of Gold(I) Thiomalate (Myocrisin) Including Applications to Cysteine Derivatives. *Dalton Trans.* **1982**, 135–141.
25. Uson, R.; Laguna, A.; Laguna, M.; Briggs, D.A.; Murray, H.H.; Fackler, J.P. (Tetrahydrothiophene) Gold(I) or Gold(III) Complexes. In *Inorganic Syntheses*; John Wiley & Sons, Inc.: Hoboken, NJ, USA, 2007; pp. 85–91.
26. Bordwell, F.G.; Hughes, D.L. Thiol Acidities and Thiolate Ion Reactivities toward Butyl Chloride in Dimethylsulfoxide Solution—The Question of Curvature in Bronsted Plots. *J. Org. Chem.* **1982**, *47*, 3224–3232.